NUCL SCI TECH (2019) 30:66
https://doi.org/10.1007/s41365-019-0578-2

# Generation of two-color polarization-adjustable radiation pulses for storage ring light source

**Wei-Hang Liu[1,2] · Yi Wu[2] · Yi Jiao[1] · Zheng-He Bai[3] · Sheng Wang[4]**

Received: 8 August 2018 / Revised: 16 September 2018 / Accepted: 9 October 2018 / Published online: 22 March 2019


**Abstract** To date, two-color pulses are widely used in pump–probe experiments. For a ring-based light source, the power of the spontaneous radiation fluctuates randomly in the longitudinal direction. It is difficult to produce two-color double pulses by optical methods. In this paper, we introduce a method based on the echo-enabled harmonic generation scheme that generates two-color pulses in a storage ring light source. By adopting crossed undulators and a phase shifter, the polarization of the two-color pulses can be easily switched. A numerical simulation based on a diffraction-limited storage ring, the Hefei Advanced Light Source, suggests that the time delay and spectral separation of the two pulses can be adjusted linearly by changing the pulse duration and chirp parameters of the seed laser. A circular polarization degree above 80% could be achieved.

This work was supported by the National Natural Science Foundation of China (Nos. 11475202, 11405187), Youth Innovation Association of Chinese Academy of Sciences, and Bureau of Frontier Sciences and Education, Chinese Academy of Sciences (No. QYZDJ-SSW-SLH001), and National Key R&D Program of China (No. 2016YFA0401900).

✉ Yi Jiao
jiaoyi@ihep.ac.cn

1 Key Laboratory of Particle Acceleration Physics and Technology, Institute of High Energy Physics, Chinese Academy of Sciences, Beijing 100049, China

2 University of Chinese Academy of Sciences, Beijing 100049, China

3 National Synchrotron Radiation Laboratory, University of Science and Technology of China, Hefei 230029, China

4 China Spallation Neutron Source, Institute of High Energy Physics, Chinese Academy of Sciences, Dongguan 523803, China

**Keywords** Two-color pulses · Echo-enabled harmonic generation · Diffraction-limited storage ring · Crossed undulators · Circular polarization

## 1 Introduction

Two-color radiation pulses with different wavelengths and an adjustable time delay have been widely used in pump–probe experiments. Two different optical pulses are injected into the sample that is to be studied. One of these is called the pump pulse and is meant to prepare the system in a specific state, e.g., revert the system to optical transparency. The second pulse is called the probe pulse and is captured after it has travelled through the sample. Then, analysis of this probe pulse yields information about the state of the system [1], and by controlling the polarization of the radiation pulses, it is possible to investigate the dynamic processes occurring during a series of chemical reactions [2].

Many two-color pulse generation methods for linac-based free-electron lasers (FELs) have been proposed and demonstrated experimentally. The first two-color FEL in the soft X-ray region was realized at the Linac Coherent Light Source using the emittance spoiler method [3], double undulator method [4], and fresh-slice method [5]. In these methods, the FEL operates in the self-amplified spontaneous emission (SASE) [6] mode. Note that, the FEL can also be operated in the seeded mode by using seeding techniques such as the high-gain harmonic generation (HGHG) scheme [7] or the echo-enabled harmonic generation (EEHG) scheme [8, 9], which can be used to improve the longitudinal coherence of the SASE–FEL. Another two-color pulse generation method for FELs is operation in the seeded mode based on the HGHG scheme, which is called the chirped seed laser method [10–13]. In this method, a seed laser with a linear frequency chirp is adopted to generate double FEL pulses with different wavelengths. The APPLE-type undulator method [14, 15] or the crossed undulator method [16–20] can be applied to control the polarization of the radiation pulses. It is easier to switch the helicity of the radiation pulses in the crossed undulator method, which uses two undulators with orthogonal magnetic fields than in the APPLE-type undulator method. An adjustable magnetic chicane (phase shifter) is installed between the two undulators to change the arrival time difference between the electron beam and the radiation field, and consequently the phase difference between the two radiation fields. In this way, arbitrarily polarized light can be obtained.

Given the high repetition rate and stability of electron beams in a storage ring (SR), it is attractive and useful to generate two-color polarization-adjustable pulses in SRs. To generate two-color radiation pulses in SRs, the method based on HGHG requires a high modulation energy. High energy modulation will increase the energy spread of the SR beam (by approximately one order), making the beam unstable in the SR, and the harmonic conversion number will be low ($<10$). Because the seed wavelength is in the ultraviolet region, the output radiation is limited to the extreme ultraviolet region. EEHG can generate higher harmonic radiation (up to 1 nm) with low energy modulation and has been extensively studied in SRs to generate coherent radiation [21–24]. To generate two-color radiation pulses in the soft X-ray region, the EEHG scheme is adopted. To flexibly adjust the polarizability of the two-color pulses, the crossed undulator method is used. The modulated beams travel through two undulators and generate two coherent radiation pulses. The two radiation pulses have different polarization directions and are superimposed to form circularly polarized light. The degree of polarization can be adjusted by a phase shifter in the central region of the radiator. In the following sections, the details of the proposed method and the simulation results are presented.

The remainder of this paper is organized as follows. In Sect. 2, the methods of generating two-color radiation pulses in SRs are introduced. A numerical simulation of this method based on the Hefei Advanced Light Source (HALS) [25, 26] is described in Sect. 3. Section 4 demonstrates the simulation results of polarization control at HALS. The conclusions are provided in Sect. 5.

## 2 Methods

The layout of the proposed method is illustrated schematically in Fig. 1. The EEHG structure is located in two adjacent straight sections. The electron beam interacts with the first laser in the first undulator (mod 1), gaining energy modulation. After passing through the arc between the two straight sections, the electron beam is over-compressed on the laser wavelength scale, forming an energy band structure in longitudinal phase space. Then, the electron beam gains energy modulation from a frequency-chirped laser in the second undulator (mod 2), where the energy modulation is converted to density modulation in the dispersion section (chicane). Two-color pulses are generated when finishing the transportation to the downstream undulator (radiator). Considering that the sign of $R_{56}$ element of the chicane is opposite to that of the arc section, the conditions for parameter optimization of the EEHG scheme are different from those used in the FEL. The optimization scheme for this case has been described in detail in Ref. [24]. We will review the main points below. The bunching factor in a one-dimensional (1-D) approximation can be written as

$$b_{nm} = |\exp\{[-(1/2)nB_1 + (m+n)B_2]^2\} \\ J_m[-(m+n)A_2B_2]J_n\{-A_1[nB_1 + (m+n)B_2]\}|, \tag{1}$$

where $n$ and $m$ are integers; $A_i = \Delta\gamma_i/\sigma_\gamma$ and $B_i = R_{56}^{(i)}k_s\sigma_\gamma/\gamma$ are dimensionless parameters with $i = 1, 2$; $\Delta\gamma$ and $\sigma_\gamma$ are the energy modulation amplitude and beam

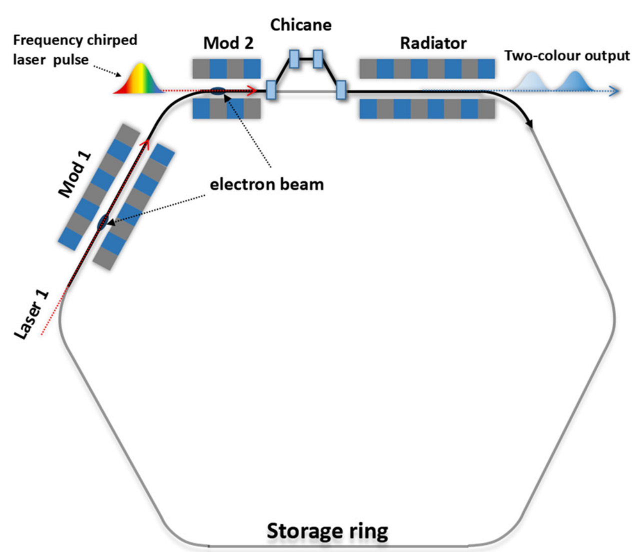


**Fig. 1** (Color online) Layout of two-color method in an SR: The modulator and radiator are placed on the adjacent straight sections. A laser with a linear frequency chirp is adopted as the second modulation laser

energy spread, respectively; $R_{56}^{(i)}$ is the longitudinal dispersion in the arc region ($i = 1$) or the chicane ($i = 2$); $k_s = 2\pi/\lambda_s$, where $\lambda_s$ is the wavelength of the seed lasers (two seed lasers with the same wavelength); and $\gamma$ is the Lorentz factor of the electron beam. In this case, the optimal conditions for maximizing the bunching factor are $B_1 \times B_2 < 0$, $n = 1$, and $m > 0$ [24]. The optimal conditions for $A_2$, $B_2$ are

$$\begin{cases} \xi opt = B_1 + NB_{2,\mathrm{opt}} \\ A_{2,\mathrm{opt}} = \dfrac{N - 1 + 0.81(N-1)^{1/3}}{NB_{2,\mathrm{opt}}}, (N > 5), \end{cases} \quad (2)$$

where $N$ is the harmonic conversion number, and $B_1$ is a constant related to the arc design of the SR. $\xi opt$ maximizes $F(\xi, A_1) = J_1(\xi A_1)\exp(-\xi^2/2)$ at a specific $A_1$. Given $A_1$, $B_1$, and $N$, the optimal values of $A_2$ and $B_2$ can be obtained by solving Eq. (2).

The SR EEHG operates in the coherent radiation regime. In this regime, the maximal bunching factor is determined by the parameters $A_1$, $A_2$, $B_1$, and $B_2$. The radiation power is proportional to the square of the bunching factor [27]. We may attempt to find the properties of the two-color pulses by analyzing the time distribution of the optimal bunching factor.

Given a laser having a Gaussian power profile with duration $\sigma_t$, the dimensionless energy modulation amplitude $A$ can be written as

$$A(t) = A_0 \exp\left(\frac{-t^2}{4}\right), \quad (3)$$

where $A_0$ is the maximal value of $A(t)$, and $t$ is the time coordinate in unit of $\sigma_t$.

Assuming the first laser has a longer duration than the second laser, the first energy modulation amplitude $A_1$ can be considered independent of time, and $A_2(t)$ obeys Eq. (3). Combining Eqs. (1) and (3) yields the time distribution of the bunching factor:

$$b_N(t) = \left| J_{N-1}\left[NB_2A_2\exp\left(\frac{-t^2}{4}\right)\right] J_1[A_1\xi]\exp\left(\frac{-\xi^2}{2}\right)\right|, \quad (4)$$

where $\xi = B_1 + NB_2$. By giving $A_1$ and letting $\xi$ maximize $F(\xi, A_1)$, the scale function of the bunching factor can be obtained:

$$B_N(t) = \frac{b_N(t)}{F(\xi, A_1)} = \left| J_{N-1}\left[\phi_N \exp\left(\frac{-t^2}{4}\right)\right]\right|, \quad (5)$$

where $\phi_N = NB_2A_2$.

$B_N(t)$ is the absolute value of the $(N-1)$th-order Bessel function with argument $\phi_N \exp(-t^2/4)$. Taking $N = 60$, the corresponding $B_{60}(t)$ for various $\phi_{60}$ values was calculated, as shown in Fig. 2.

Figure 2 shows two symmetrical peaks with a time interval of $\Delta t = 1.04\sigma_t$ when $\phi_{60} = 66.5$. Two coherent radiation pulses with an interval of $\Delta t$ would be generated after the modulated electron beam passes through the radiator.

In general, the bunching factor could generate two symmetrical peaks along the longitudinal direction when $\phi_N$ is the first positive zero point $r_1$ of Bessel function $J_{N-1}(x)$. According to the properties of Bessel functions, $(N-1)$th-order Bessel function reaches the first maximum when

$$x = N - 1 + 0.81(N-1)^{1/3}. \quad (6)$$

If we let $x = r_1 \exp(-t^2/4)$, we find that the time interval of the pulses obeys the relation

$$\Delta t = 4\sigma_t \sqrt{\ln\left(\frac{r_1}{N - 1 + 0.81(N-1)^{1/3}}\right)}. \quad (7)$$

The spectral distance between the two radiation pulses with time interval $\Delta t$ is

$$\Delta\omega = 2N\Delta t\alpha, \quad (8)$$

where $\alpha$ is the linear frequency chirp of the second seed laser.

Equations (7) and (8) indicate that the time interval and spectral distance of the pulses are linearly proportional to the duration $\sigma_t$ and the frequency chirp $\alpha$ of the second seed laser. Thus, the time interval and spectral distance of the radiation pulses can be adjusted linearly by controlling the parameters of the seed laser.

To control the polarization of the two-color pulses, the crossed undulator method was adopted (Fig. 3). The crossed undulators are composed of radiator-H, with a

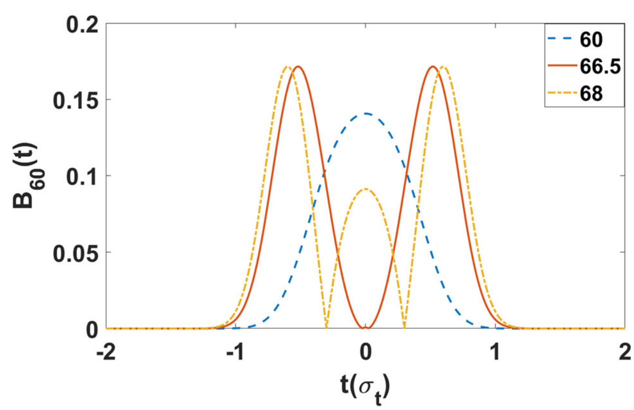


**Fig. 2** (Color online) Curve of $B_{60}(t)$ for various $\phi_{60}$ values

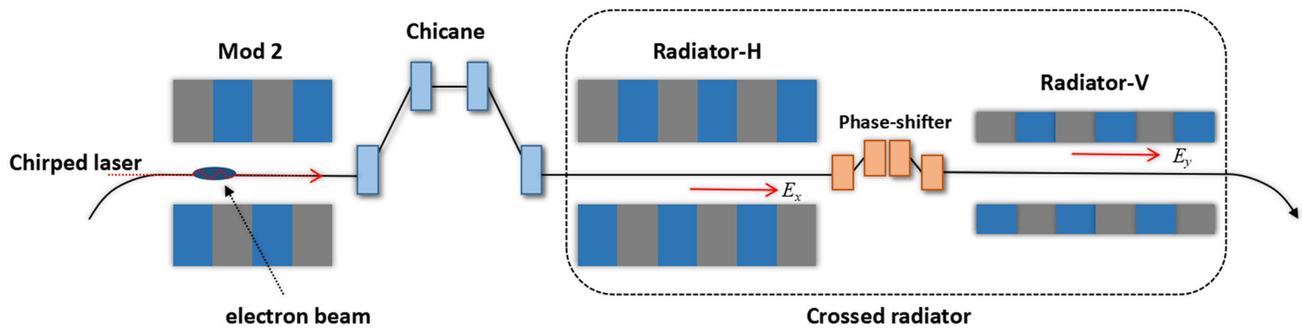


**Fig. 3** (Color online) Schematic of the polarization adjustment method. The phase shifter is used to shift the path delay between the electrons and the radiation pulse

magnetic field in the horizontal direction, and radiator-V, with a magnetic field in the vertical direction.

The polarization of the radiation output can be characterized by the Stokes parameters, which are defined as [28]

$$\mathbf{S} = \begin{pmatrix} s_0 \\ s_1 \\ s_2 \\ s_3 \end{pmatrix} = \begin{pmatrix} \langle E_x^2 \rangle + \langle E_y^2 \rangle \\ \langle E_x^2 \rangle - \langle E_y^2 \rangle \\ 2\langle E_x E_y \cos(\Delta\phi) \rangle \\ 2\langle E_x E_y \sin(\Delta\phi) \rangle \end{pmatrix}, \tag{9}$$

where angle brackets $\langle ... \rangle$ indicate averaging over time. $E_x$ and $E_y$ are the electric fields with $x$ and $y$ polarization, respectively. The degrees of the total and circular polarization are

$$Ptot = \frac{\sqrt{s_1^2 + s_2^2 + s_3^2}}{s_0} \tag{10}$$

and

$$Pcir = \frac{|s_3|}{s_0}. \tag{11}$$

From Eqs. (10) and (11), one can see that the maximized polarization can reach 100% when $E_x$ and $E_y$ are the same in the temporal and spectral domains. By adjusting the phase difference between $E_x$ and $E_y$, one can realize circular polarization from 0 to 100%.

## 3 Two-color operation of HALS

A case study of the proposed method based on HALS is given in this section to demonstrate its feasibility. HALS was put forward some years ago as a future soft X-ray diffraction-limited SR at the National Synchrotron Radiation Laboratory in China.

The simulation results of two-color pulses in the water window region (4 nm) are presented below. The seed laser wavelength was 240 nm, with $B_1 = -20.3$, $A_1 = 3$, and $N = 60$. The interaction between the electron beam and laser in the undulator was simulated using GENESIS [29], and the output electron beam distribution data were utilized in ELEGANT [30] to simulate the electron beam passing through the arc section in HALS. The acquired longitudinal distribution of the beam in phase space is shown in Fig. 4. The energy band structure can be seen clearly. From Eq. (2), the optimal values of $A_2$ and $B_2$ are 2.99 and 0.35, respectively. The 1-D analysis on which the results are based differs from the three-dimensional (3-D) situation, so the bunching factors (Fig. 5) are calculated using GENESIS with various values of $B_2$ and $A_2$ for parameter accuracy. The corresponding optimal $A_2$ and $B_2$ values are 3.13 and 0.293, respectively. According to the first section, the parameter $\phi_N = NB_2A_2$ needs to have an appropriate value for the bunching factor to obey a bimodal distribution and generate dipulse radiation. The theoretical value of $\phi_{60}$ is 66.5, according to 1-D analysis. Allowing for the 3-D effect, we calculate the bunching factor distributions corresponding to various $\phi_{60}$ values using GENESIS by changing $A_2$ (Fig. 6).

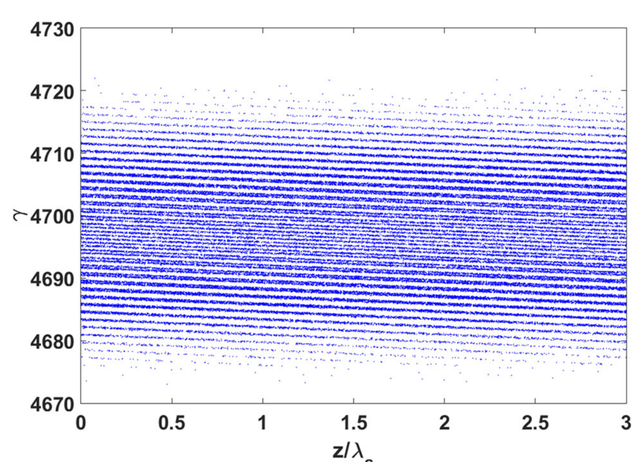


**Fig. 4** (Color online) Longitudinal distribution of electron beam in phase space after the arc region

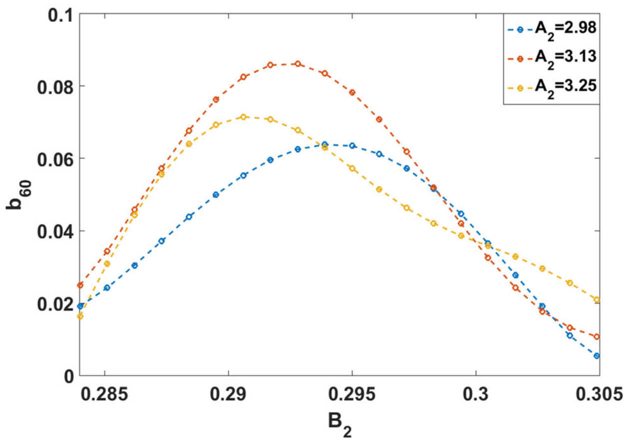


**Fig. 5** (Color online) Bunching factor for various values of $A_2$ and $B_2$

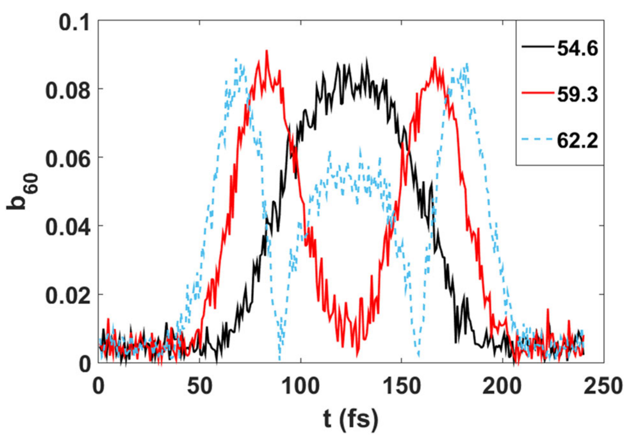


**Fig. 6** (Color online) Curve of $b_{60}(t)$ for various $\phi_{60}$ values calculated by GENESIS

The theoretical results from Sect. 2 neglect the beam emittance and the nonlinear terms of the beam line, so they deviate from the simulation results. We find that the simulation result for $\phi_{60}$ is smaller than the theoretical result. As can be seen from Fig. 6, when $\phi_{60} \approx 59.3$ and $A_2 \approx 3.4$, the bunching factor follows a bimodal distribution. The specific parameters are listed in Table 1. The transition from single-pulse to double-pulse behavior is not sudden, so the optimal value of $\phi_{60}$ is defined as the value at which the power of the suppressed emission from the central part of the electron bunch is negligible compared to that of the two peaks. For example, in this paper, we take the bunching factor for the central part of the electron bunch to be less than 0.02, so the peak power of the double pulse is more than 16 times the power of the central part of the electron bunch. Two-color radiation pulses are simulated using the parameters in Table 1, among which the second seed laser pulse duration is 100 fs, and the frequency chirp $\alpha$ is $1.22 \times 10^{26}\ \mathrm{fs}^{-2}$. The simulation result is presented in Fig. 7. Gaussian-like dipulses are generated

**Table 1** Main parameters of the proposed method at HALS

| Parameter | Value |
|---|---|
| Beam energy (GeV) | 2.4 |
| Energy spread (%) | 0.08 |
| Bunch length (mm) | 2.07 |
| Horizontal emittance (pm · rad) | 21 |
| Vertical emittance (pm · rad) | 2.1 |
| Peak current (A) | 12 |
| Length of the straight section (m) | 5.1 |
| Period of mod 1, mod 2 (m) | 0.2, 0.2 |
| Radiator period (cm) | 2 |
| Radiation wavelength (nm) | 4 |
| Peak power of seed laser 1 (GW) | 3.38 |
| Peak power of seed laser 2 (GW) | 7.1 |
| Rayleigh length of seed lasers 1, 2 (m) | 4, 2 |
| Seed wavelength (nm) | 240 |
| Arc region $R_{56}$ (mm) | − 0.945 |
| Chicane $R_{56}$ (μm) | 13.40 |
| Chicane length (m) | 1.072 |
| Period number of mod 1, mod 2 | 20, 10 |
| Period number of radiator | 50 |

with a time separation of 103 fs, and the durations of the first and second pulses are 21 and 22 fs, respectively. The spectral separation of the first and second pulses is 0.98 eV.

To verify the accuracy of Eqs. (7) and (8), the radiation dipulse interval $\Delta t$ and the energy separation of the central photons $\Delta E = \hbar\Delta\omega$, which correspond to seed lasers with various pulse durations and frequency chirps, are calculated (Fig. 8). $\hbar$ is the reduced Planck constant. In Fig. 8, good agreement between the linearized solution of Eqs. (7) and (8) and the simulation results can be observed.

To intuitively demonstrate the longitudinal distribution of the radiation pulses, the Wigner function $W(\omega, t)$ [31] is used:

$$W(\omega, t) = \int E^*\left(t + \frac{\tau}{2}\right)E\left(t - \frac{\tau}{2}\right)\exp(-i\omega\tau)\,\mathrm{d}\tau, \qquad (12)$$

where $E(t)$ is the electric field of the radiation pulse, $E^*(t)$ is the complex conjugation of $E(t)$, and $\omega$ is the radiation frequency.

Figure 9a, b shows the Wigner distributions of radiation pulses with the same $\Delta E$, 1.6 eV, but different time intervals: $\Delta t = 40$ fs (a) and $\Delta t = 80$ fs (b). The simulation results with the same time interval, $\Delta t = 50$ fs, but different energy separations, $\Delta E = 0.6$ eV and $\Delta E = 1.2$ eV, are shown in Fig. 9c, d, respectively. Figure 9 clearly shows that the frequency and time of the output pulses are linearly correlated.

In order to change the pulse duration online, a few methods can be applied to change the pulse duration from

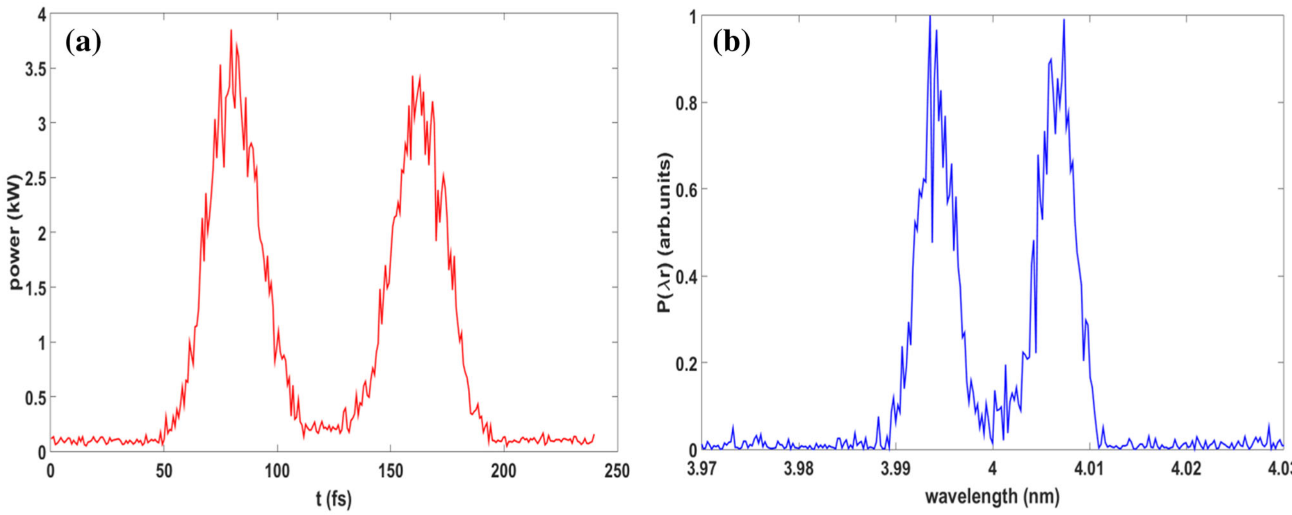


**Fig. 7** Distribution of the two-color radiation output in time domain (**a**) and spectral domain (**b**)

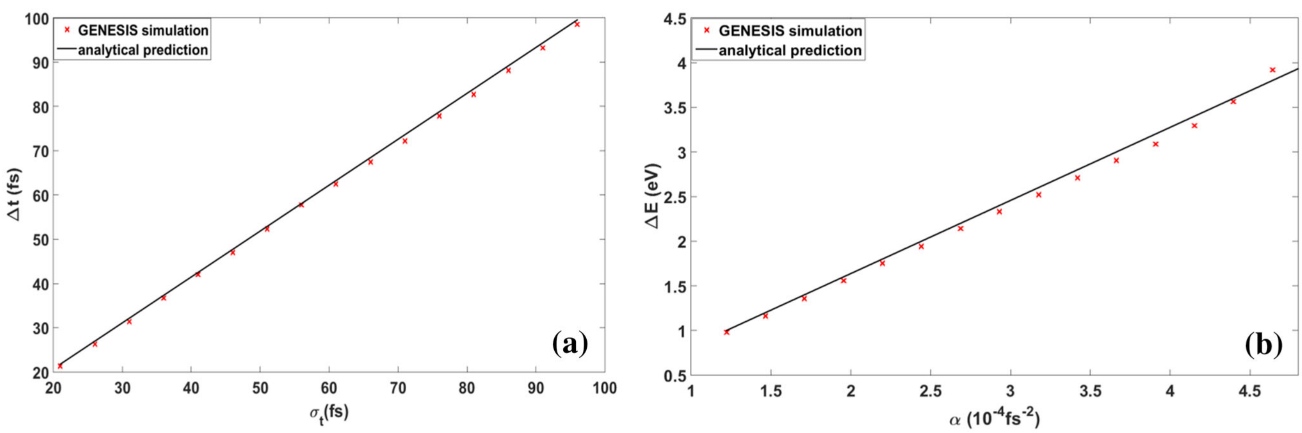


**Fig. 8** Time interval variation over seed pulse duration at $\Delta E = 1$ eV (**a**) and central energy separation over seed laser chirp at $\Delta t = 104$ fs (**b**)

hundreds of femtoseconds to dozens of picoseconds, such as combining multiple lasers and introducing a delay between the Q-switched pulses of each laser [32, 33], or controlling the variation in spectral bandwidth via a tunable filter [34]. A controllable frequency chirp can be induced by propagating the seed pulse through a stretcher [35]. The linear frequency chirp can be continuously tuned by changing the parameters of the stretcher.

## 4 Polarization control at HALS

To obtain polarization-adjustable radiation pulses, we adopt the crossed undulator method by separating the 1-m-long radiator into two 0.5-m-long radiators, radiator-H and radiator-V. A 0.3 m phase shifter is placed in the center to control the polarization. The layout is shown in Fig. 3.

To realize perfect circular polarization, the radiation from the two crossed radiators should overlap perfectly in the temporal and spectral domains. This is difficult to achieve in practice. To maximize the coincidence of the pulses in the temporal and spectral domains, the optimal bunching factor (see Fig. 6, red line) is realized at the center of the phase shifter by slightly changing the parameter $B_2$. As a result, the radiation pulses from radiator-H and radiator-V will overlap in the temporal and spectral domains. The output radiation pulses are shown in Fig. 10. It can be seen that the polarization pulses in the two directions are similar in shape and intensity. However, they are not exactly the same, for it is impossible to ensure that radiation pulses produced by two coherent radiation processes are identical. Moreover, because of the slippage effect in radiator-H and the phase shifter, the two pulses do not completely overlap in the time domain.

$Ptot$ and $Pcir$ are shown in Fig. 11. We can see that the total polarization degree is approximately 85%, and the degree of circular polarization reaches its maximum when the phase is close to $0.3\pi + n\pi$, where $n$ is an integer.

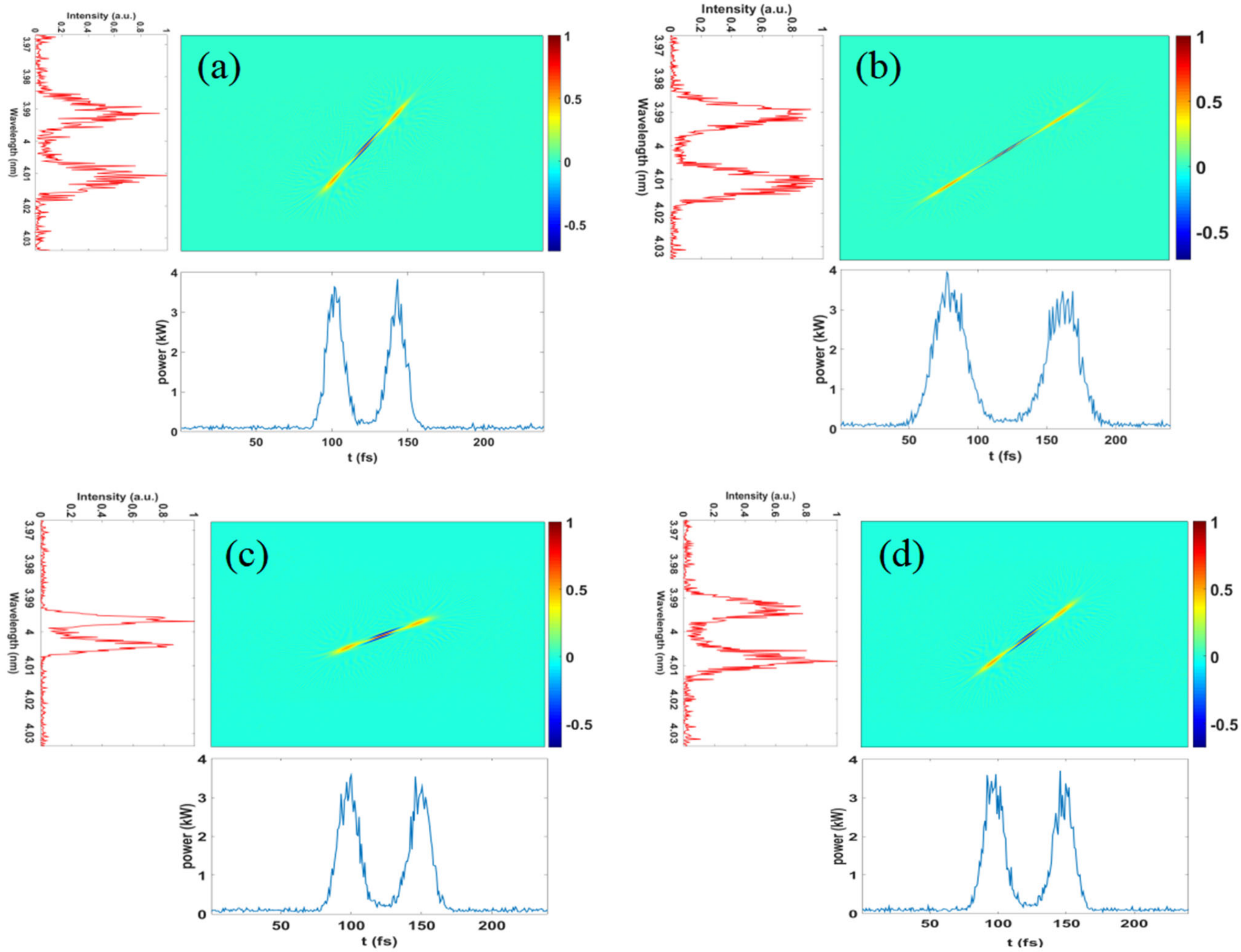

**Fig. 9** (Color online) Wigner distributions of the simulation results under different conditions

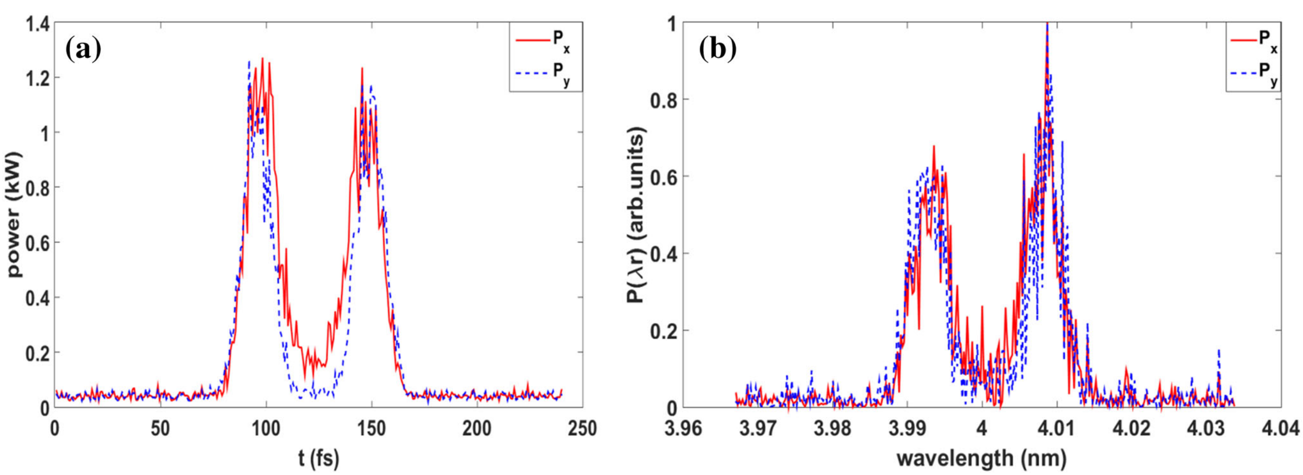

**Fig. 10** (Color online) Radiation pulses in the time domain (**a**) and the frequency domain (**b**)

It can be concluded from the theoretical and simulation results that a stable dipulse duration and delay can be produced when $\phi_{60}$ stabilizes around an appropriate value. In order to obtain dipulse peaks with powers greater than 5 times the power in the central part of the dipulse, the parameters should be set to $57.2 < \phi_{60} = 60AB < 61.4$.

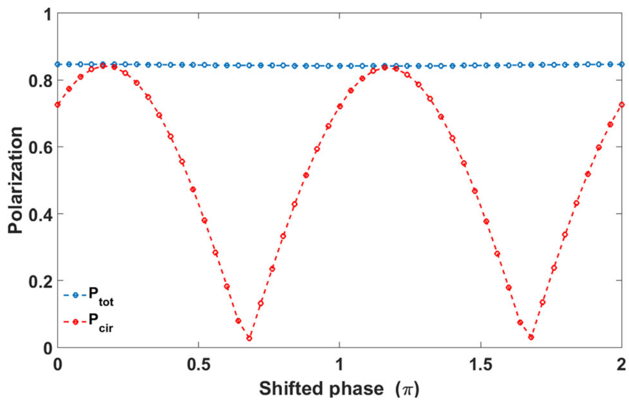


**Fig. 11** (Color online) Polarization degree variation with phase shifter tuning

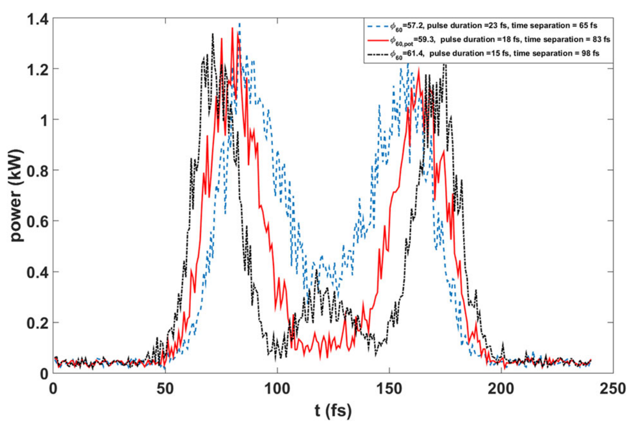


**Fig. 12** (Color online) Radiation pulses in the time domain for various $\phi_{60}$ values

$\Delta A/A + \Delta B/B = \Delta(AB)/(AB) = \Delta(\phi_{60})/(\phi_{60}) < 3.5\%$ could be obtained, which means that the sum of the fluctuations in the chicane parameters and energy modulation should be less than 3.5%. If the shot-to-shot fluctuation of the laser power is 5%, it can be obtained that $\Delta A/A \approx 2.5\%$, and $\Delta B/B$ increases to 1%. This indicates that the fluctuation of the magnetic field in the chicane should be better than 1%. As shown in Fig. 12, the largest change rates of the dipulse duration and delay are approximately 20%.

## 5 Conclusion

By adopting a chirped seed laser in the EEHG scheme, we achieved two-color coherent radiation pulses with a peak power of approximately 1.2 kW in an SR. The time delay and spectral separation of the two pulses can be adjusted linearly by changing the pulse duration and chirp parameters of the seed laser. Using crossed undulators and a phase shifter, a circular polarization degree above 80% was achieved. This method provides a way to supply two-color polarization-adjustable pulses to ring-based light sources. The peak power density of the dipulse is approximately 30 MW/cm$^2$, which is much larger than that of the synchrotron radiation background. Therefore, this scheme is more applicable to experiments in which the electric field threshold of the pump–probe system is larger than the electric field produced by synchrotron radiation.

The disadvantage of this scheme is that different intervals would result in different pulse durations, which is a common problem for the single-bunch and single seed laser chirp methods. Therefore, this scheme cannot be applied to experiments that are sensitive to the pump–probe pulse duration.

Although the simulation in this paper assumes a diffraction-limited SR, this method is feasible for existing third-generation SR light sources. The principal experimental proof of this method is easy to implement in existing SRs. We expect the proposed method to provide stable two-color pulses at SR light sources for pump–probe experiments in the near future.

**Acknowledgements** The authors thank Guanqun Zhou at IHEP, Tong Zhang at FRIB, Ling Zeng, and Gang Zhao at Peking University for helpful discussions.

## References


1. A. Röhm, *Dynamic Scenarios in Two-State Quantum Dot Lasers: Excited State Lasing, Ground State Quenching, and Dual-Mode Operation* (Springer, Berlin, 2015)
2. H. Anetai, T. Takeda, N. Hoshino et al., Circular polarized luminescence of hydrogen-bonded molecular assemblies of chiral pyrene derivatives. J. Phys. Chem. C **122**, 6323 (2018). https://doi.org/10.1021/acs.jpcc.7b12747
3. P. Emma, K. Bane, M. Cornacchia et al., Femtosecond and subfemtosecond X-ray pulses from a self-amplified spontaneous-emission-based free-electron laser. Phys. Rev. Lett. **92**, 074801 (2004). https://doi.org/10.1103/PhysRevLett.92.074801
4. A.A. Lutman, R. Coffee, Y. Ding et al., Experimental demonstration of femtosecond two-color X-ray free-electron lasers. Phys. Rev. Lett. **110**, 134801 (2013). https://doi.org/10.1103/PhysRevLett.110.134801
5. A. Lutman, T. Maxwell, J. MacArthur et al., Fresh-slice multi-colour X-ray free-electron lasers. Nat. Photon. **10**, 745 (2016). https://doi.org/10.1038/nphoton.2016.201
6. R. Bonifacio, C. Pellegrini, L.M. Narducci, Collective instabilities and high-gain regime free electron laser. AIP Conf. Proc. **118**, 236 (1984). https://doi.org/10.1063/1.34640
7. L.H. Yu, Generation of intense UV radiation by subharmonically seeded single-pass free-electron lasers. Phys. Rev. A **44**, 5178 (1991). https://doi.org/10.1103/PhysRevA.44.5178
8. G. Stupakov, Using the beam-echo effect for generation of short-wavelength radiation. Phys. Rev. Lett. **102**, 074801 (2009). https://doi.org/10.1103/PhysRevLett.102.074801
9. D. Xiang, G. Stupakov, Echo-enabled harmonic generation free electron laser. Phys. Rev. Spec. Top. Accel. Beams **12**, 030702 (2009). https://doi.org/10.1103/PhysRevSTAB.12.030702

10. E. Allaria, R. Appio, L. Badano et al., Highly coherent and stable pulses from the FERMI seeded free-electron laser in the extreme ultraviolet. Nat. Photon. **6**, 699 (2012). https://doi.org/10.1038/nphoton.2012.233
11. E. Allaria, F. Bencivenga, R. Borghes et al., Two-colour pump–probe experiments with a twin-pulse-seed extreme ultraviolet free-electron laser. Nat. Commun. **4**, 2476 (2013). https://doi.org/10.1038/ncomms3476
12. B. Mahieu, E. Allaria, D. Castronovo et al., Two-colour generation in a chirped seeded free-electron laser: a close look. Opt. Express **21**, 22728 (2013). https://doi.org/10.1364/OE.21.022728
13. C. Feng, Z. Wang, X. Wang et al., Generation of two-color ultrashort radiation pulses from two electron bunches and a chirped seeded free-electron laser. Nucl. Inst. Methods Phys. Res. A **807**, 79 (2016). https://doi.org/10.1016/j.nima.2015.11.001
14. S. Sasaki, Analyses for a planar variably-polarizing undulator. Nucl. Inst. Methods Phys. Res. A **347**, 83 (1994). https://doi.org/10.1016/0168-9002(94)91859-7
15. J. Bahrdt, W. Frentrup, A. Gaupp et al., Magnetic field optimization of permanent magnet undulators for arbitrary polarization. Nucl. Inst. Methods Phys. Res. A **516**, 575 (2004). https://doi.org/10.1016/j.nima.2003.08.155
16. K.J. Kim, A synchrotron radiation source with arbitrarily adjustable elliptical polarization. Nucl. Inst. Methods Phys. Res. A **219**, 425 (1984)
17. K.J. Kim, Circular polarization with crossed-planar undulators in high-gain FELs. Nucl. Inst. Methods Phys. Res. A **445**, 329 (2000). https://doi.org/10.1016/S0168-9002(00)00137-6
18. Y. Ding, Z. Huang, Statistical analysis of crossed undulator for polarization control in a self-amplified spontaneous emission free electron laser. Phys. Rev. Spec. Top. Accel. Beams **11**, 030702 (2008). https://doi.org/10.1103/PhysRevSTAB.11.030702
19. H. Geng, Y. Ding, Z. Huang, Crossed undulator polarization control for X-ray FELs in the saturation regime. Nucl. Inst. Methods Phys. Res. A **622**, 276 (2010). https://doi.org/10.1016/j.nima.2010.07.050
20. H. Deng, T. Zhang, L. Feng et al., Polarization switching demonstration using crossed-planar undulators in a seeded free-electron laser. Phys. Rev. Spec. Top. Accel. Beams **17**, 020704 (2014). https://doi.org/10.1103/PhysRevSTAB.17.020704
21. R. Molo, M. Höner, H. Huck et al., EEHG and Femtoslicing at DELTA, in *Proceedings of FEL2013*, New York, USA, pp. 594–597 (2013)
22. C. Evain, A. Loulergue, A. Nadji et al., Soft X-ray femtosecond coherent undulator radiation in a storage ring. New J. Phys. **14**, 023003 (2012). https://doi.org/10.1088/1367-2630/14/2/023003
23. W. Gao, H. Li, L. Wang, Preliminary study of EEHG-based superradiant undulator radiation at the HLS-II storage ring. Chin. Phys. C **41**, 078101 (2017). https://doi.org/10.1088/1674-1137/41/7/078101
24. W. Liu, G. Zhou, Y. Jiao, Generating femtosecond coherent X-ray pulses in a diffraction-limited storage ring with the echo-enabled harmonic generation scheme. Nucl. Sci. Tech. **29**, 143 (2018). https://doi.org/10.1007/s41365-018-0476-z
25. N. Hu, Z.H. Bai, W. Li et al., Estimates of collective effects in the HALS storage ring having the first version lattice, in *Proceedings of IPAC2017*, Copenhagen, Denmark, pp. 3770–3773 (2017)
26. Z.H. Bai, W. Li, L. Wang et al., Design of the second version of the HALS storage ring lattice, in *Proceedings of IPAC2018*, Vancouver, BC, Canada, pp. 4601–4604 (2018)
27. L. Yu, J. Wu, Theory of high gain harmonic generation: an analytical estimate. Nucl. Instrum. Methods Phys. Res. Sect. A **483**, 493 (2002). https://doi.org/10.1016/S0168-9002(02)00368-6
28. M. Born, W. Emil, *Principles of Optics* (Cambridge University Press, Cambridge, 2009)
29. S. Reiche, GENESIS 1.3: a fully 3D time-dependent FEL simulation code. Nucl. Inst. Methods Phys. Res. A **429**, 243 (1999). https://doi.org/10.1016/S0168-9002(99)00114-X
30. M. Borland, Elegant: A flexible SDDS-compliant code for accelerator simulation, Advance Photon Source. United States: N. p. (2000). https://doi.org/10.2172/761286
31. E. Wigner, On the quantum correction for thermodynamic equilibrium. Phys. Rev. **40**, 749 (1932). https://doi.org/10.1103/PhysRev.40.749
32. N. Hay, I. Baker, Y. Guo et al., Stability-enhanced, high-average power green lasers for precision semiconductor, in *Processing in Solid State Lasers XXI: Technology and Devices* (Vol. 8235, p. 82351E)
33. M. Poulter, N. Hay, B. Fulford et al., Q-switched Nd: YAG lasers for high average-power and high peak-power operation, in *Processing in Solid State Lasers XVIII: Technology and Devices* (Vol. 7193, p. 719309)
34. D. Li, H. Jussila, Y. Wang et al., Wavelength and pulse duration tunable ultrafast fiber laser mode-locked with carbon nanotubes. Sci. Rep. **8**, 2738 (2018). https://doi.org/10.1038/s41598-018-21108-3
35. E. Treacy, Optical pulse compression with diffraction gratings. IEEE J. Quantum Electron. **5**, 454 (1969). https://doi.org/10.1109/JQE.1969.1076303